Biodecolorization of Remazol dyes using biochar derived from *Ulva reticulata:* isotherm, kinetics, desorption, and thermodynamic studies

A.K. Priya[a], R. Gokulan[b,*], A. Vijayakumar[b], S. Praveen[b]

[a]*Department of Civil Engineering, KPR Institute of Engineering and Technology, Coimbatore, Tamil Nadu 641 407, India, email: akpriy@gmail.com (A.K. Priya)*
[b]*Department of Civil Engineering, GMR Institute of Technology, Rajam, Andhra Pradesh 532 127, India, Tel. +91-9944233081; emails: gokulravi4455@gmail.com/gokulan.r@gmrit.edu.in (R. Gokulan), vijayakumarkct@gmail.com (A. Vijay Kumar), praveensarvan@gmail.com (S. Praveen)*

ABSTRACT

In this work, the preliminary batch trials were performed to optimize the factors influencing the Remazol dyes remediation using *Ulva reticulate* biochar. *U. reticulate* a green marine seaweed is used as a low-cost adsorbent to remediate the Remazol dyes in aqueous solution. The optimum values were achieved at 2 g/L biochar dosage, 2.0 equilibrium pH, 0.05 mmol/L initial dye concentration, and 30°C temperature with a maximum removal efficiency of around 92%. Thermodynamic studies proved that the reactions are spontaneous and endothermic. Toth a three-parameter isotherm model performed well in comparison with other models demonstrating a regression coefficient of 0.9999. The kinetic study results indicate that the pseudo-second-order kinetic is the best fit model. Finally, the regeneration study concluded that of different elutant, NaOH showed the maximum desorption efficiency of greater than 99.2% for all four Remazol dyes.

Keywords: *Ulva reticulate* derived biochar; Isotherm; Kinetics; Remazol dye; Sorption

1. Introduction

Dyes are classified based on their application characteristics as direct, acid, disperse, basic, reactive, mordant, sulfur, and disperse. Dyes are available as azo, nitro, acridine, carotenoid, indamine, diphenylmethane, xanthene, phthalocyanine, anthraquinone, indigoid, quinoline, inorganic pigment, sulfur, etc., based on chemical structure. Dyes can also be categorized as cationic, anionic, and non-ionic colors based on the structure [1].

The estimated annual production of dyes is around 7,000–10,000 kilotons [2]. The global use of reactive dyes is continuously increasing to meet demand. On the other hand, dye bearing wastewater generated from industries is having the worst impact on the environment [3]. In textile industries during the dyeing process, some quantity of applied dyes is not utilized. Based on the type of fabrics water demand may vary, a total of 0.08–0.15 m³ of water is utilized per kg of fabric production. Wastewater about 1,000–3,000 m³ is discharged after treatment of approximately 12–20 tons of fabrics per 24 h [4,5]. Dyes are commonly toxic and cause health issues [6]. Synthetic dyes are commonly removed by physical methods [7,8]. Some chemical methods like chemical oxidation involve the use of chemicals for the transformation of pollutants, but the recent approach for the remediation of dyes is based on the biological method [9,10].

As reported by Vijayaraghavan and Yun [11] and Malik [12] numerous biological ways are available to treat inorganic and organic pollutant-containing wastewaters, these include

* Corresponding author.

biosorption, biodegradation, bioaccumulation, bioleaching, phytoremediation, bio-sparging, bio-augmentation, bioventing, and bio-stimulation. Of these methods, many researchers centered on biosorption, biodegradation, phytoremediation, and bio-accumulation for dye-containing wastewaters as they proved efficient in dye remediation from contaminated waters [11].

Biochar is obtained from waste materials through thermal degradation in the absence of O$_2$ (pyrolysis). Experimental outcomes by Nartey and Zhao [13] portray that the selection of proper feedstock is crucial for biochar preparation as it greatly influences the functional groups, pores, and other adsorption properties of biochar. Biochar is generally produced from biological materials, which are acquired at low or nil cost [14]. Application of biochar for the water and wastewater treatment is the recent approach and the adsorption of these pollutants is maximum when compared to other types of bio sorbents. Biochar can be prepared for any waste materials that are rich in carbon content and numerous studies have been carried out using biochar produced for agricultural waste (rice husk, coconut shell, groundnut shell, etc.). But the synthesis of biochar from the seaweeds is very much limited and to the best of our knowledge, this is the first attempt that involves the utilization of biochar produced from green seaweed (*Ulva reticulata)* for the remediation of Remazol dyes. Green seaweeds are very common in the southern parts of India and its alternative usage in environmental remediation is on the horizon. Hence, the current research examines the potential of biochars, synthesized from locally available marine green algae (*U. reticulata),* towards sorption.

2. Materials and methods

2.1. Seaweed and Remazol dyes

Green marine seaweeds (*U. reticulate)* are harvested from Rameswaram, India. The Remazol dyes were procured from Sigma-Aldrich, India and the properties of the Remazol dyes used in this study are shown in Table 1.

2.2. Thermal pyrolysis

Distilled water is used to wash the collected marine algae and subsequently dried naturally for 24 h. Approximately, the collected biomass is crushed and it is sieved to a particle size of 0.75 mm. The sieved biomass was heated in the muffle furnace (Make: ANTSLD) (300°C–500°C) at the heating rate of 5°C/min for 120 min [15]. The oxygen-free environment is maintained in the muffle furnace by applying 100 mL/min of N$_2$ gas for 10 min [16]. Once the pyrolysis is completed,

the muffle furnace was allowed to cool to reach room temperature and the resulting biochar is stored in desiccator [16]. Three trials were carried out for each pyrolysis temperature to obtain the average results. The biochar yield is calculated by using Eq. (1).

$$Biochar\ Yield\left(\%\right)=\left(\frac{m_1}{m_2}\right)\times 100 \tag{1}$$

where m_1 is the mass of the biochar after thermal degradation (kg or g), m_2 is the mass of the raw biomass before thermal degradation (kg or g).

2.3. Biochar characterization

An elemental analyzer (2400 Series II-PerkinElmer, USA) was used to determine the elemental profile of biochar. Moisture content, ash content, fixed carbon content, and volatile matter content were determined using proximate analysis [17]. Scanning electron microscopy (Hitachi, USA – S4800) was used to study the surface characteristics of biochar and FT-IR spectrophotometer (Bruker, USA – attenuated total reflectance infra red (ATR IR)) was used to analyze major shifts occurred in functional groups of biochar samples. Before analyzing, the dried biochar samples were mixed with potassium bromide (KBr) to form pellets.

2.4. Batch experiments

Batch studies were carried with a volume of 100 mL in an Erlenmeyer flask (250 mL). A rotary orbital shaker is used for mixing the content at 160 rpm. The contact time of 8 h is established to reach equilibrium conditions. A centrifuge is used to separate the dye-bounded biochar from the solution and it is carried out at 3,000 rpm for 5 min [18]. A spectrophotometer is used to find the final concentration of the dyes. The batch studies were carried out by varying biochar dosage, pH, temperature, and initial solute concentration.

2.5. Influence of biochar dosage, pH, temperature, and initial solute concentration

The impact of different parameters on the removal of Remazol dye was studied by varying biochar dosage (1–10 g/L), pH (1.75–5.0), temperature (20°C–45°C) and initial dye concentration (0.05–1 mmol/L).

2.6. Isotherm and kinetic studies

Freundlich and Langmuir (two-parameter isotherm model), Sips and Toth (three-parameter isotherm model)

Table 1
Characteristics of Remazol dyes

Dyes	Empirical formula	Color index	Molecular weight (g/mol)	λ_{max} (nm)
Remazol brilliant blue R (RBBR)	$C_{22}H_{16}N_2Na_2O_{11}S_3$	61,200	626.54	595
Remazol brilliant orange 3R (RBO3R)	$C_{20}H_{17}N_3Na_2O_{11}S_3$	17,757	617.54	490
Remazol brilliant violet 5R (RBV5R)	$C_{20}H_{16}N_3Na_3O_{15}S_4$	18,097	735.58	577
Remazol black B (RBB)	$C_{26}H_{21}N_5Na_4O_{19}S_6$	20,505	991.82	597

were studied. Kinetic study is carried out by varying the initial concentration (0.1, 0.25, 0.5, 0.75, and 1.0 mmol/L) at varying time intervals (10, 20, 30, 40, 50, 60, 90, 120, 180, 240, 300, and 360 min) [19].

2.7. Thermodynamic studies

Thermodynamic properties such as standard free energy, standard enthalpy, and standard entropy were evaluated under 293, 303, and 313 K using Eqs. (2) and (3).

$$\Delta G° = -RT \ln K_L \qquad (2)$$

$$\Delta G° = \Delta H° - T\Delta S° \qquad (3)$$

where $DG°$ is the standard free energy, $DH°$ is the standard enthalpy, $DS°$ is the standard entropy, K_L is the Langmuir constant (L/mol), T is the temperature in K, and R is the gas constant (kJ/mol/K).

The value of $DH°$ and $DS°$ were calculated from the slope ($-DH°/R$) and intercept ($DS°/R$) of the plot of $\ln K_L$ vs. $1/T$ [20].

2.8. Desorption studies

In an attempt to study the practicability of recycling the spent biochar for another cycle of sorption, several eluting agents were employed to elute the attached dye molecules from the utilized biochar. For desorption (elution) experiments, dye-laden biochar in a 250 mL Erlenmeyer flask was bought into contact with 100 mL of different elutant. The elutant used in the present study include 0.1 M NaOH, Na_2CO_3, NH_4OH, HCl, CH_3OH, and ethylenediaminetetraacetic acid (EDTA). The influence of solid/liquid (S/L) ratio on the desorption potential of adsorbent was determined by the varying volume of elutant used. Once the elution process was concluded, the dye-free biochar was extensively rinsed with deionized water and subsequently contacted with 0.5 mmol/L of Remazol dye solution. After equilibrium attainment, the biochar was separated from the suspension and subjected to desorption. This process of sorption–elution was conducted continuously for three cycles to assess the regeneration potential of biochar.

3. Results and discussion

3.1. Influence of pyrolysis temperature

Fig. 1 shows that the increase in temperature reduces the yield of the biochar. Similar results have been reported by Becidan et al. [21] and Tan et al. [22]. This is because at elevated temperature seaweed biomass will undergo higher decomposition that will result in the degradation of the elemental composition of the biomass. So, it is concluded that the biochar samples produced at 300°C were selected as the optimum and used for further studies.

3.2. Characterization of biochar

Analyse of an elementary profile of *U. reticulata* derived biochar (ultimate analysis) showed that the increase in temperature decreased the biochar yield. Generally, at elevated
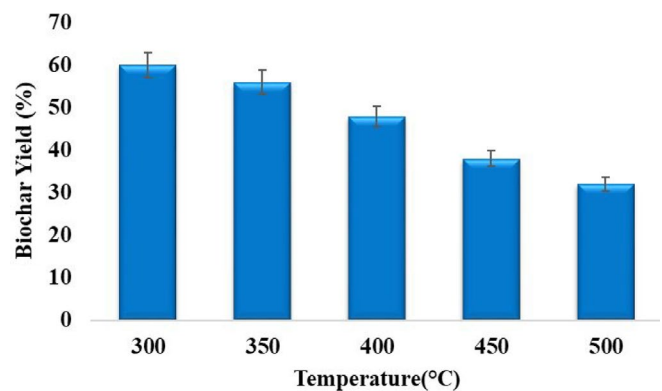

Fig. 1. Effect of different temperature on biochar yield.

temperature, biochar yield decreases and bio-oil and biogas yield will increase [13]. The maximum carbon content of 31.2% is attained at a temperature of 300°C, whereas carbon content of 24.6% is attained at a temperature of 500°C. The increase in temperature from 300°C to 500°C has decreased the carbon yield of about 6.6%. From Table 2, it is also evident that the increase in temperature decreased H (%), O (%), N (%), and S (%) content. So, the optimum pyrolysis temperature is considered as 300°C for the production of maximum biochar yield. The proximate analysis of *U. reticulata* showed moisture content of 18.20%, ash content of 14.71%, volatile matter of 28.15%, and fixed carbon content of 62.14%.

Fig. 2 shows the SEM images of raw *U. reticulata*, biochar of *U. reticulate*, and Remazol dye-loaded samples. In general, uneven pores with different sizes were identified over the biochar surface and favored the derived biochar to act as an adsorbent. SEM images proved that the biochar after dye sorption turned to a smooth surface, which indicates that the impurities are removed during the dye sorption process in acidic conditions [19].

From the Brunauer–Emmett–Teller analyze, the surface area of raw and biochar of *U. reticulate* is found to be 172.50 and 345.50 m²/g, the pore volume is found to be 0.112 cm³/g (raw) and 0.334 cm³/g (biochar), pore radius is found to be 12.21 Å (raw), and 19.41 Å (biochar). From the result, it is evident that *U. reticulata* derived biochar is having high potential in adsorption than the raw *U. reticulata*.

Fig. 3 shows the FT-IR spectra of strong bands for *U. reticulate* derived biochar. FT-IR spectra of biochar derived from *U. reticulate* confirmed the presence of strong bands such as alcohol (C–O and –OH stretching), carboxyl ((C=O) symmetric and C=O stretch of COOH, asymmetric), aromatic (C–H stretch), and amine (N–H stretch). From Table 3, it is also concluded that there is a shift in the functional group of Remazol dye loaded biochar and this may be due to the ion exchange between sorbent and dyes used. Hence, the FT-IR data revealed the binding of Remazol dyes is due to the functional groups present in the biochar.

3.3. Influence of biochar dosage

The biochar dosage was varied from 1 to 10 g/L (with a fixed pH (2), initial dye concentration (0.5 mmol/L), and

Table 2
Ultimate analysis of biochar prepared from *Ulva reticulate* at different pyrolysis temperatures

Biochar	Temperature (°C)	C (%)	H (%)	O (%)	N (%)	S (%)
U. reticulata- derived biochar	300	31.2 ± 1.2	3.6 ± 0.2	24.6 ± 0.8	4.4 ± 0.2	5.9 ± 0.8
	350	29.1 ± 1.3	3.2 ± 0.3	23.5 ± 0.9	4.3 ± 0.2	5.2 ± 0.2
	400	27.6 ± 1.1	2.9 ± 0.2	22.6 ± 1.2	3.9 ± 0.1	4.6 ± 0.2
	450	25.4 ± 0.9	2.3 ± 0.1	22.1 ± 1.3	3.5 ± 0.1	3.8 ± 0.1
	500	24.6 ± 0.4	1.5 ± 0.1	16.5 ± 0.6	2.7 ± 0.1	3.2 ± 0.2

Mean ± SD

temperature (30°C)) to study the optimum dosage. Fig. 3 shows the effect of biochar dosage on the dye uptake capacity. The adsorption capacity of various Remazol dyes decreased to 79% with an increase in biochar dosage up to 10 g/L. At lower dosage, all the binding sites will be effectively utilized for the adsorption process, with an increase in dosage the binding sites get increased and that results in agglomeration. This leads to a decline in the uptake capacity of the biochar [24]. Whereas, the removal efficiency increases from 36.6% to 79.6% (RBB), 41.6% to 86.4% (RBV5R), 45.0% to 95.8% (RBO3R), and 43.8% to 91.8% (RBBR) while, sorbent dosage is increased from 1 to 10 g/L. A sorbent will have a sufficient surface area to bind the ions present in the dye molecules at a high dose [25]. So, from the batch studies, 2 g/L is considered as the optimum biochar dosage.

3.4. Influence of equilibrium pH

The pH ranges from 1.75 to 5.0 are selected to study the effect of pH in the adsorption process. Fig. 4 proved that an increase in pH decreased the uptake capacity. In high acidic conditions, the enhancement of Remazol dye sorption was due to interactions of sorbent and other anions (dyes). These reactive dyes exist in solution as negative colored ions, thus interacting with positively charged sorbent surfaces, which favors the binding of dyes at a lower pH of 2. From the results, the optimum pH for the sorption of Remazol dye is 2. A similar study was carried out by Vijayaraghavan and Ashokkumar [26] and reported that the optimum pH is 2.0 for the removal of Remazol brilliant blue R (Reactive dye) using biochar derived from marine seaweed.

3.5. Influence an increase in biochar dosage temperature

Temperature between 25°C and 45°C is maintained to study the effect on the adsorption process. The biochar dosage, equilibrium pH and initial concentration are kept constant at 2 g/L, 2, and 0.05 mmol/L. From the batch studies, it is clear that removal efficiency increases with an increase in temperature. The maximum removal efficiency obtained at 45°C and 35°C for four dyes were in the order of RBO3R (89.8% and 87.8%), RBBR (86.8% and 85%), RBV5R (83.4% and 81.4%), and RBB (73.8% and 71.2%). The difference in removal efficiency between 45°C and 30°C is found to be less than 2% for all dyes. So, in economic aspects and favorable environmental conditions, 30°C is fixed as the optimum for the adsorption process.

3.6. Sorption isotherms

Isotherm experiment is carried out to predict the absorption potential of the sorbent [27]. The initial concentration of 0.05, 0.10, 0.25, 0.50, 0.75, and 1 mmol/L, at constant temperature (30°C), biochar dosage (2 g/L), and pH (2.0) is used to study the effect of experimental uptake with the predicted uptake of different isotherm models. Table 4 shows, that an increase in initial concentration increased the uptake capacity of sorbent. However, at higher concentrations, the uptake capacity is saturated with very little increase in the uptake capacity. At an initial concentration of 1 mmol/L, the maximum experimental uptake capacities were estimated as 0.281 (RBO3R), 0.273 (RBBR), 0.253 (RBV5R), and 0.207 (RBB) mmol/g. Whereas, for an initial concentration of 0.05 mmol/L the maximum uptake capacity (mmol/g) was estimated as 0.0229 (RBO3R), 0.0226 (RBBR), 0.0215 (RBV5R), and 0.021 (RBB). From the results, it is also calculated that the maximum percentage uptake capacity of adsorbate was estimated as 22.9% (RBO3R), 22.55% (RBBR), 21.5% (RBV5R), and 20.99% (RBB) for 0.05 mmol/L. whereas it is estimated as 14.025% (RBO3R), 13.625% (RBBR), 12.66% (RBV5R), and 10.35% (RBB) for 1 mmol/L. So, based on the uptake by adsorbate, it is concluded that optimum initial concentration is 0.05 mmol/L.

The uptake capacity is compared with the two-parameter and three-parameter isotherm models to understand the correlation between experimental uptake and predicted uptake by isotherm models. Fig. 5 shows the experimental uptake and predicted uptake of different isotherm models. Sathishkumar et al. [28] reported that the Freundlich model can be used only for low to intermediate ranges and the Langmuir model assumes that the sorbent is sorbed to the adsorbent by physical forces in general and that all binding groups have the same affinity to the adsorbent [29].

Of all the isotherm models, prediction by the Toth model is well in accordance with the experimental values with the lowest average % error values (<3.81%) and the highest correlation coefficient values (>0.997). Similar to experimental uptake (Q_e) the uptake capacity predicted (Q_{Cal}) by the Toth model was also found to be maximum for RBO3R, and minimum for RBB.

3.7. Sorption kinetics

The process conditions for the kinetic studies are carried out by varying the dye concentration (0.1–1 mmol/L) with a fixed pH of 2.0 and a temperature of 30°C. The contact time is playing an important role in kinetic studies.
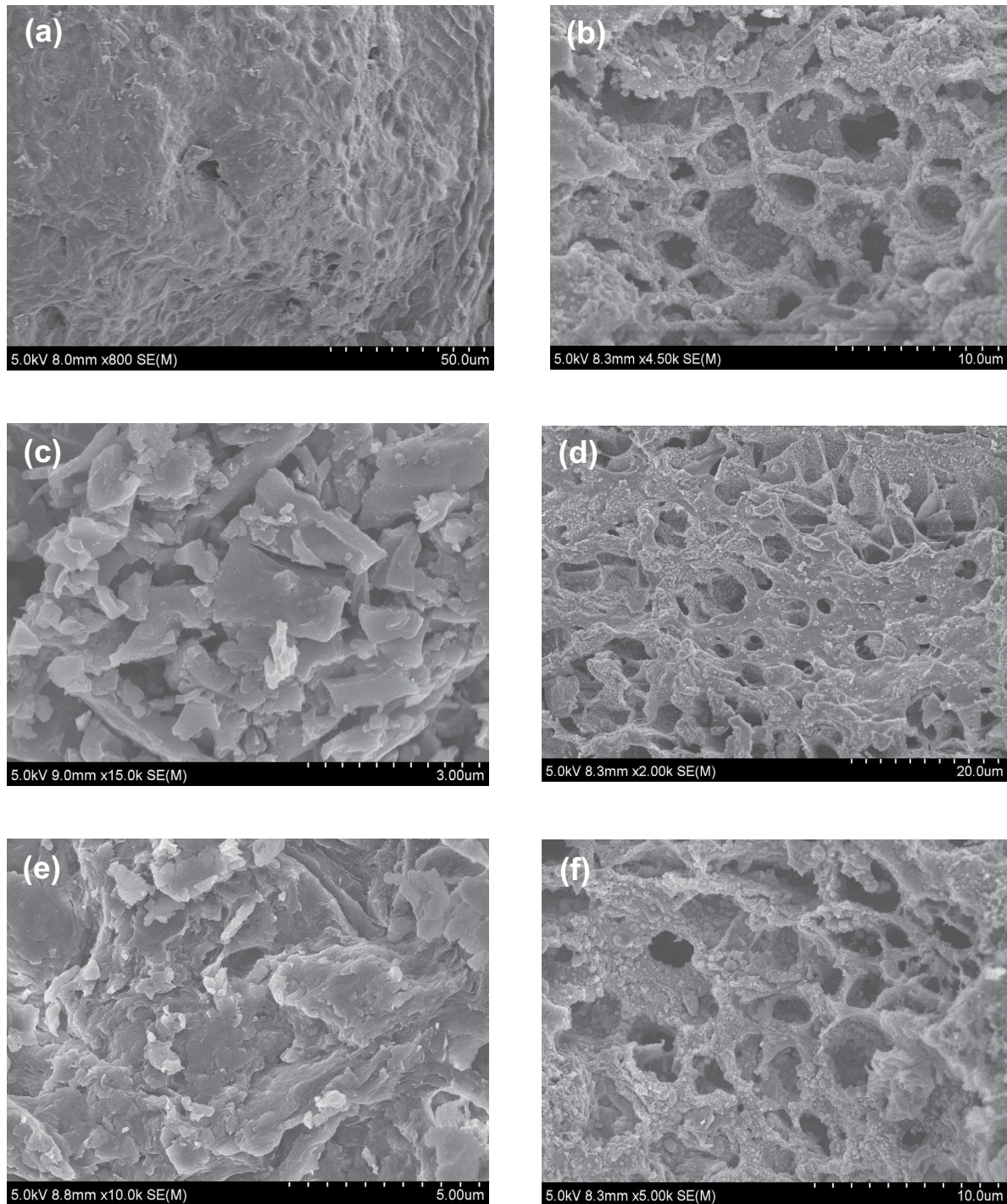
Fig. 2. Scanning electron micrographs of *Ulva reticulata* (a), *Ulva reticulata*-derived biochar (b), RBB-loaded biochar (c), RBV5R-loaded biochar (d), RBO3R-loaded biochar (e), and RBBR-loaded biochar (f) [23].

From Fig. 6, it is evident that during the kinetic study, the dye sorption capacity was high for the first 60 min and with an increase in contact time, the sorption capacity is reduced. Since 0.1 mmol/L achieved 90% of total sorption in 60 min whereas, it took 120 min for an initial concentration of 1 mmol/L. from the kinetic studies, it is also concluded that the equilibrium contact time was estimated as 300 min. In an attempt to evaluate the kinetic data, the pseudo-first and pseudo-second-order kinetic models were utilized. The pseudo-first-order model provided better results as shown in Table 5. Based on high R^2 and low percentage error values, the pseudo-second-order kinetic model's prediction was better than the pseudo-first-order model. (Table 5). It should also be noted that the adsorption
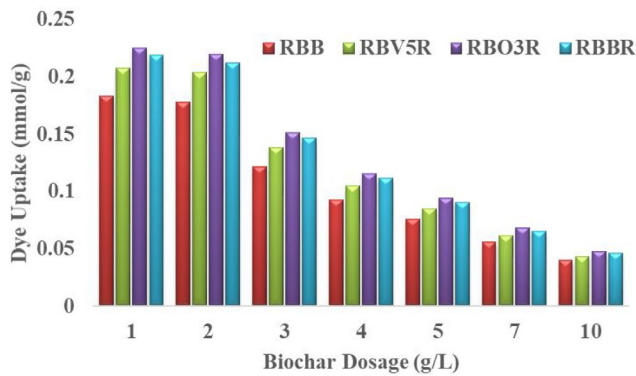
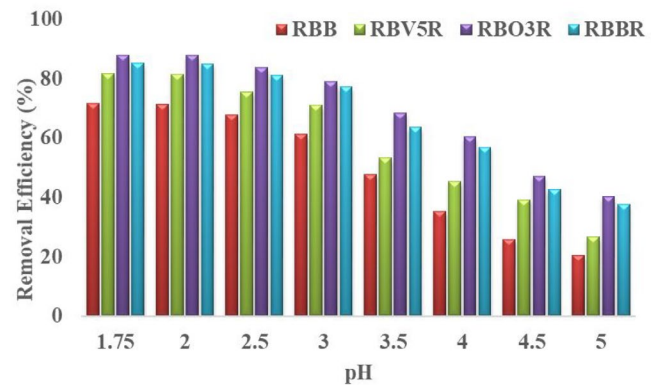Fig. 3. Effect of biochar dosage on uptake capacity of *U. reticula-ta*-derived biochar for Remazol dyes.

Fig. 4. Effect of solution pH on the removal efficiency of *U. reticulata*-derived biochar for Remazol dyes.

capacity predicted by the pseudo-second-order model was higher than the experimental uptakes (Table 5), which indicates that the biochar exhibits substantial surface heterogenicity [30]. It also reveals that boundary layer thickness and external mass transfer strongly influences the adsorption, without resistance to mass transfer within the pores of the sorbent. Moreover, adsorption on boundary layer is strongly governed by the electron-donor forces between these anionic dyes and positively charged biochar [31,32]. This is agreeable with the results obtained from the effect of pH, since the optimum pH for the removal of Remazol dyes is 2, which indicates the surface of the biochar is charged with positive ions (H^+) that enhance the maximum removal efficiency. The uptake of each dye concerning the time at varying initial concentrations is shown in Fig. 6.

3.8. Thermodynamic studies

Thermodynamic parameters were calculated by carrying out experiments at three different temperatures (293, 303, and 313 K). From the plot $\ln K_L$ vs. $1/T$, it is possible to calculate the thermodynamic parameters. Table 6 demonstrates the thermodynamic parameters for four Remazol dyes at different temperatures (293, 303, and 313 K). The $+DH°$ indicates that the reaction is endothermic and it also indicates that the chemical behavior of Remazol dyes by biochar, from which the Remazol dyes stay bound to

U. reticulata derived biochar surface groups with strong interactive forces, nearly as a chemical bond [33]. Similarly, a positive value of $DS°$ reflects the adsorbent's affinity to the adsorbed species that shows a certain degree of disorder over Remazol dye – biochar interface, which may be related to heterogeneous multilayer character of the adsorption since Toth model fits the experimental data. The $DG°$ was found to be negative for all three temperatures and reveals that reactions are spontaneous at all temperatures. The negative (–) value indicates that the reactions did not occur under a given set of conditions without intervention. These negative values also prove that chemical sorption takes place during the adsorption process [34].

3.9. Desorption studies

Desorption studies were carried out with several elutant such as Na_2CO_3, NH_4OH, 0.01 M NaOH, EDTA, CH^3OH, and HCl. From the results, it is concluded that alkaline mediums performed well in desorption studies when compared to the acidic mediums. For instance, the maximum desorption efficiency observed was 99.3%, 98.1%, and 90.7% in the case of NaOH, Na_2CO_3, and NH_4OH when employed for RBB-loaded *U. reticulata* derived biochar. Acidic elutant such as HCL, CH_3OH, and EDTA were performed with a very low desorption efficiency of less than 2.7% (Fig. 7). This may be because desorption is the reversible reaction of adsorption.

Table 3
FT-IR spectra stretching frequencies as detected in *U. reticulata*-derived biochar and dye-bounded *U. reticulata* derived biochar [23]

Assignment	Wavenumber (cm^{-1})				
	U. reticulata-derived biochar	RBB-bounded *U. reticulata* derived biochar	RBV5R-bounded *U. reticulata* derived biochar	RBO3R-bounded *U. reticulata* derived biochar	RBBR-bounded *U. reticulata* derived biochar
C–O (alcohol) band	1,121	1,129	1,125	1,128	1,122
symmetric C=O	1,423	1,437	1,429	1,432	1,425
asymmetric C=O stretch of COOH	1,631	1,635	1,637	1,639	1,640
C–H stretch	2,984	2,981	2,985	2,984	2,988
–NH, –OH stretching	3,477	3,479	3,483	3,481	3,476

Table 4
Isotherm model parameters during adsorption of Remazol dyes by *Ulva reticulata* derived biochar

Models		RBB	RBV5R	RBO3R	RBBR
Langmuir	Q_{max}	0.2381	0.2969	0.3128	0.3101
	b_L	15.783	17.1117	29.9727	23.0724
	R^2	0.9934	0.9868	0.9874	0.9912
	% error	7.2655	12.625	15.21	11.718
Freundlich	K_F	0.2811	0.372	0.4153	0.405
	n_F	2.7501	2.6514	2.9699	2.801
	R^2	0.925	0.909	0.898	0.9108
	% error	26.691	35.522	40.728	36.791
Sips	K_S	10.878	25.7526	59.7507	31.5741
	a_S	49.8879	97.5379	210.295	112.241
	β_S	1.3108	1.4664	1.4509	1.3888
	R^2	0.9989	0.9981	0.9964	0.9997
	% error	2.35281	4.30683	5.0127	2.31254
Toth	Q_{max}	0.2106	0.254	0.2814	0.2752
	b_T	12.0179	12.2596	22.8192	17.5557
	n_T	0.5489	0.4103	0.5458	0.5389
	R^2	0.9999	0.9999	0.9968	0.9995
	% error	0.87708	0.20836	3.8102	2.0252

*Q_{max} in mmol/g; b_L in L/mmol; K_F in mmol/g $(L/mmol)^{1/n_F}$; K_S in $(L/g)_S^{\beta}$; a_S in $(L/mmol)_S^{\beta}$; b_T in L/mmol.

From the batch studies, it is found that pH 2 is the optimum and indicates that the solution is highly acidic. So, the elutant that are in acidic nature performed poor and the elutant that are in alkaline in nature performed better due to the opposite charge reactions. The S/L ratio for NaOH is further studied to calculate the effective usage of sorbent to elutant. From the result (Fig. 8), it is found that up to the S/L ratio of 5 the desorption efficiency is always greater than 99.2% for all four Remazol dyes. But, if S/L ratio is increased to 5.56, desorption efficiency is decreased to a minimum of 96.1%, 95.3%, 94.3%, and 94.8% for RBB, RBV5R, RBO3R, and RBBR. The regeneration was conducted to find the reusability of an adsorbent and three sorbent–elution cycles were employed. From the result (Fig. 9), for all the dyes, the desorption efficiency was not less than 99.1%.

4. Conclusion

The maximum removal efficiency of 91.6% is achieved for Remazol brilliant orange 3R (RBO3R) at a temperature of 30°C, pH of 2.0, biochar dosage of 2 g/L, and initial concentration of 0.05 mmol/L. Whereas the removal efficiency for RBB, RBV5R, and RBBR at the same operating conditions was found to be 83.8%, 86%, and 90.20%. The Toth model was found to be better in prediction with an R^2 value of not less than 0.9968 and % error value not greater than 3.8102. It is also concluded that the predicted uptake of isotherm models was in the order of RBO3R > RBB > RBV5R > RBBR and it is
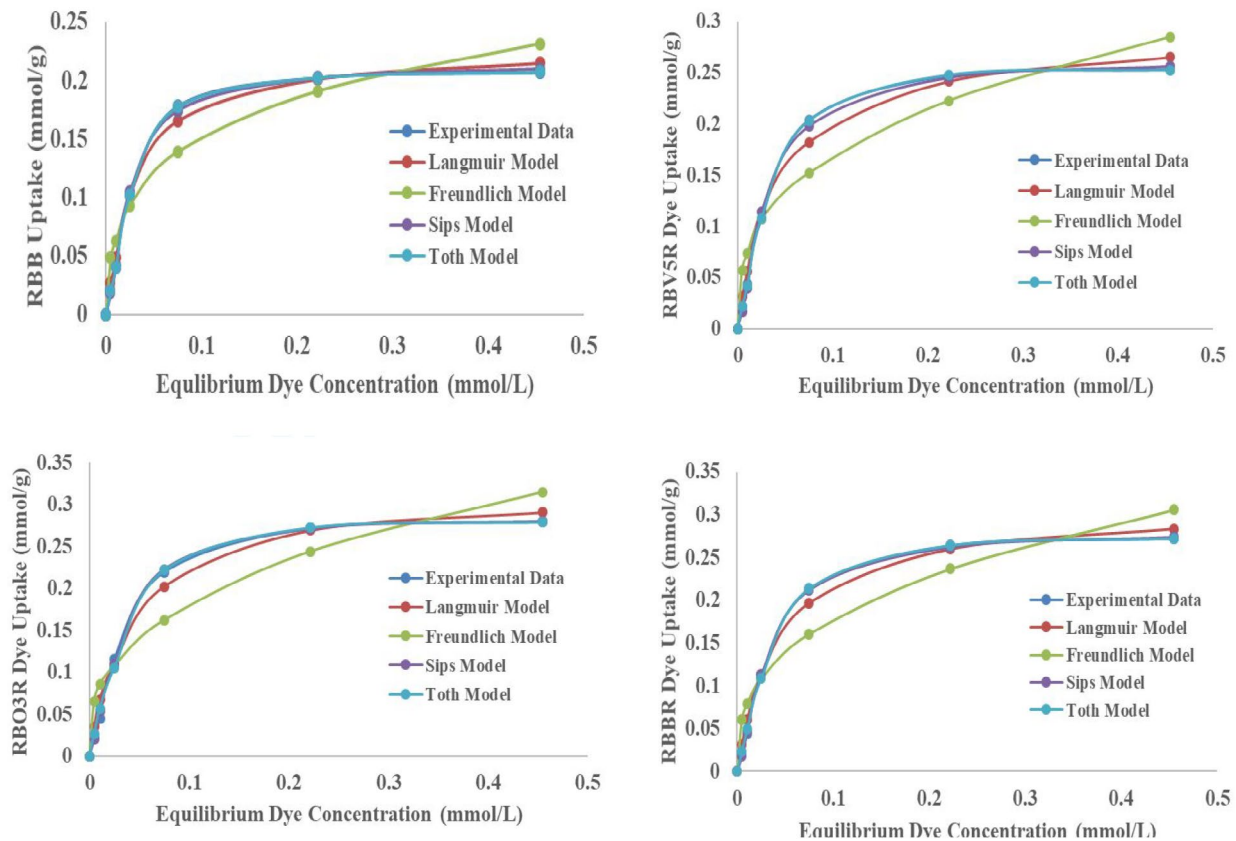

Fig. 5. Predicted dye sorption isotherms observed for RBB, RBV5R, RBO3R, and RBBR.

Table 5
Kinetic parameters of pseudo-first-order and pseudo-second-order model during sorption of Remazol dyes onto *Ulva reticulata*-derived biochar

Dyes	Model	Model constants	0.10 mmol/L	0.25 mmol/L	0.50 mmol/L	0.75 mmol/L	1.0 mmol/L
RBB		Q_e	0.0416	0.1001	0.1770	0.1990	0.1987
	Pseudo-first-order	K_1	0.0325	0.0411	0.0485	0.0526	0.0685
		R^2	0.9970	0.9979	0.9991	0.9952	0.9856
		% error	0.1089	0.6374	0.1354	0.5898	0.0821
		Q_e	0.0465	0.1102	0.1923	0.2152	0.2138
	Pseudo-second-order	K_2	0.9487	0.5373	0.3923	0.3932	0.5270
		R^2	0.9795	0.9787	0.9817	0.9924	0.9919
		% error	−1.9137	−2.2063	−1.1259	−0.4484	−0.4537
RBV5R		Q_e	0.0419	0.1051	0.2008	0.2414	0.2478
	Pseudo-first-order	K_1	0.0602	0.0630	0.0466	0.0565	0.0629
		R^2	0.9896	0.9972	0.9965	0.9876	0.9949
		% error	0.5658	0.2707	0.4972	0.3997	0.2299
		Q_e	0.0452	0.1126	0.2186	0.2609	0.2664
	Pseudo-second-order	K_2	2.1839	0.9518	0.3293	0.3500	0.3922
		R^2	0.9970	0.9877	0.9899	0.9920	0.9919
		% error	−0.2579	−0.4883	−0.7938	−0.5313	−0.5037
RBO3R		Q_e	0.0446	0.1129	0.2177	0.2644	0.2707
	Pseudo-first-order	K_1	0.0561	0.0579	0.0452	0.0541	0.0625
		R^2	0.9877	0.9888	0.9980	0.9870	0.9820
		% error	0.8084	0.6646	0.4960	0.6939	0.5856
		Q_e	0.0481	0.1215	0.2373	0.2861	0.2913
	Pseudo-second-order	K_2	1.9338	0.7910	0.2921	0.3037	0.3573
		R^2	0.9959	0.9969	0.9880	0.9971	0.9985
		% error	−0.2360	−0.1327	−0.8700	−0.2291	−0.0961
RBBR		Q_e	0.0438	0.1106	0.2121	0.2596	0.2652
	Pseudo-first-order	K_1	0.0559	0.0501	0.0421	0.0431	0.0548
		R^2	0.9892	0.9967	0.9987	0.9944	0.9903
		% error	0.6519	0.4738	0.2654	0.7203	0.6244
		Q_e	0.0472	0.1201	0.2326	0.2839	0.2868
	Pseudo-second-order	K_2	1.9434	0.6535	0.2670	0.2293	0.3079
		R^2	0.9955	0.9920	0.9781	0.9920	0.9963
		% error	−0.1790	−0.6551	−1.856	−0.7086	−0.3121

*Q_e in mmol/g; K_1 in 1/min, K_2 in g/mmol min

Table 6
Thermodynamic parameters for the adsorption of Remazol dyes by *Ulva reticulata* at different temperatures

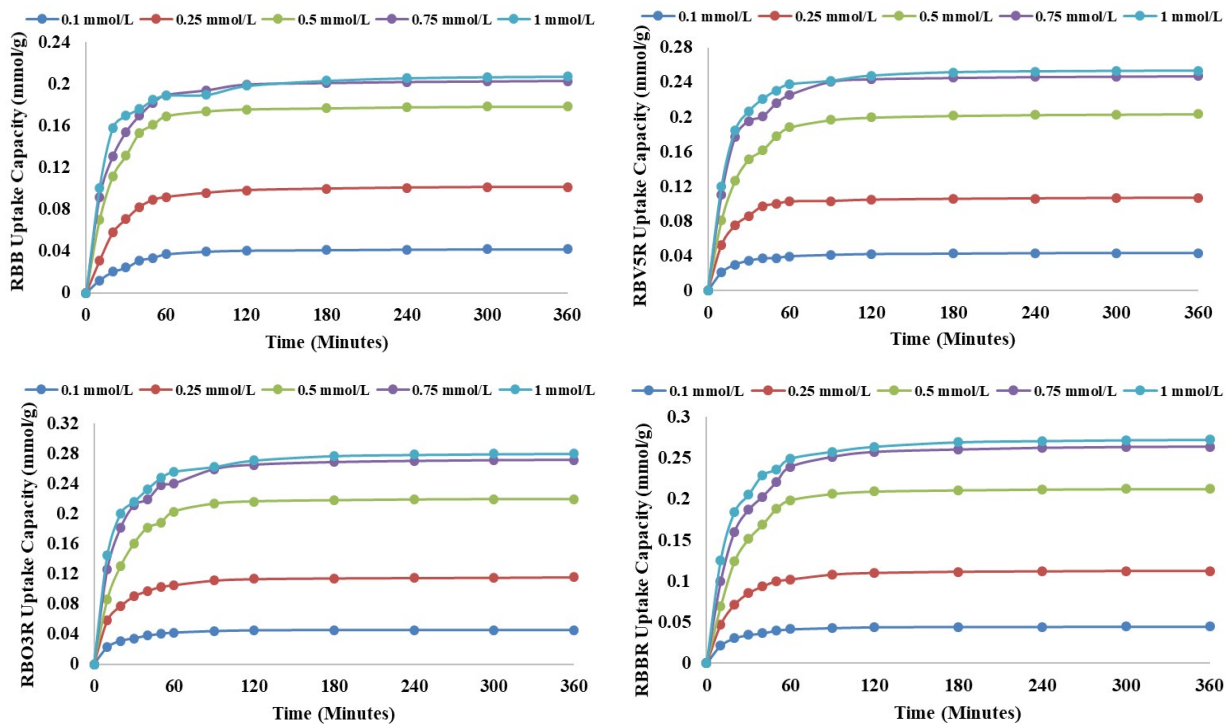| Dye	Temperature (K)	K_L (L/mol)	$\Delta G°$ (kJ/mol)	$\Delta H°$ (kJ/mol)	$\Delta S°$ (J/mol/K)
RBB	293	11,764.50	−22.83	13.74	67.69
	303	15,783.40	−24.35		
	313	16,830.50	−25.32		
RBV5R	293	12,935.97	−23.06	13.79	68.61
	303	17,113.11	−24.56		
	313	18,536.95	−25.58		
RBO3R	293	15,618.65	−23.52	27.94	118.98
	303	29,975.15	−25.97		
	313	32,314.42	−27.02		
RBBR	293	14,919.70	−23.41	22.42	99.35
	303	23,075.21	−25.31		
	313	26,786.06	−26.53		

Fig. 6. Kinetic study experimental uptake observed for different Remazol dyes.
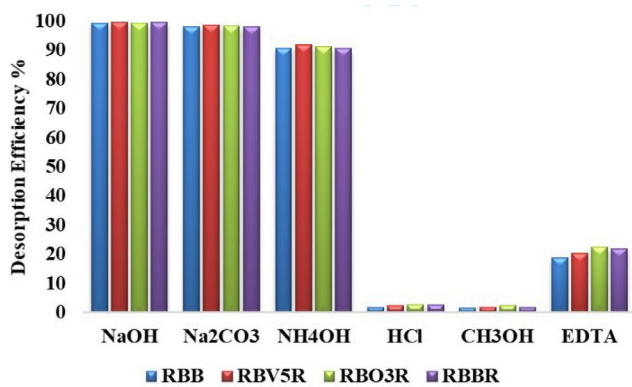

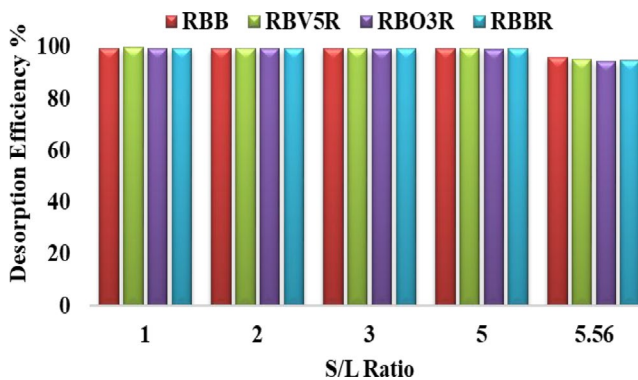Fig. 7. Desorption of Remazol dye by different elutant [23].

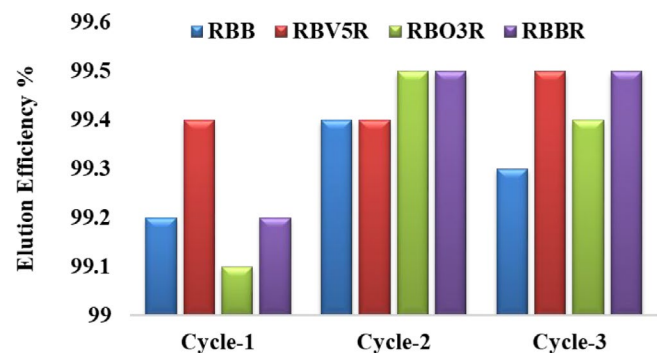Fig. 8. Impact of S/L ratio on desorption of Remazol dye [23].

Fig. 9. Sorption–elution cycle of Remazol dyes [23].

in line with experimental uptake. From the kinetics studies, it is evident that the equilibrium contact time is 300 min and second-order kinetics is found to best fit. The thermodynamic studies showed that the reactions are spontaneous and endothermic. Desorption studies proved that NaOH is the best elutant of all other elutant used and maximum desorption efficiency of 99.6% is achieved for RBV5R. From these results, it is concluded that the biochar derived from *U. reticulata* can be effectively used as an adsorbent.

References

[1] G. Mishra, M.A. Tripathy, A critical review of the treatment for decolorization of textile effluent, Colourage, 40 (1993) 35–38.
[2] V.K. Gupta, Suhas, Application of low-cost adsorbents for dye removal – a review, J. Environ. Manage., 90 (2009) 2313–2342.

[3] M. Doble, A. Kumar, Degradation of Dyes, In: Biotreatment of Industrial Effluents, Butterworth-Heinemann, Burlington, 2005, pp. 111–122.

[4] A. Al-Kdasi, A. Idris, K. Saed, C. Guan, Treatment of textile wastewater by advanced oxidation processes-a review, Global Nest J., 6 (2004) 222–230.

[5] U. Pagga, D. Brown, The degradation of dyestuffs: part II behaviour of dyestuffs in aerobic biodegradation tests, Chemosphere, 15 (1986) 479–491.

[6] I.M. Banat, P. Nigam, D. Singh, R. Marchant, Microbial decolorization of textile-dye containing effluents: a review, Bioresour. Technol., 58 (1996) 217–227.

[7] M.T. Yagub, T.K. Sen, S. Afroze, H.M. Ang, Dye and its removal from aqueous solution by adsorption: a review, Adv. Colloid Interface Sci., 209 (2014) 172–184.

[8] M.A.M. Salleh, D.K. Mahmoud, W.A.W.A. Karim, A. Idris, Cationic and anionic dye adsorption by agricultural solid wastes: a comprehensive review, Desalination, 280 (2011) 1–13.

[9] Y. Safa, H.N. Bhatti, I.A. Bhatti, M. Asgher, Removal of direct Red-31 and direct Orange-26 by low cost rice husk: influence of immobilisation and pretreatments, Can. J. Chem. Eng., 89 (2011) 1554–1565.

[10] P. Kaushik, A. Malik, Fungal dye decolourization: recent advances and future potential, Environ. Int., 35 (2009) 127–141.

[11] K. Vijayaraghavan, Y.S. Yun, Bacterial biosorbents and biosorption, Biotechnol. Adv., 26 (2008) 266–291.

[12] A. Malik, Metal bioremediation through growing cells, Environ. Int., 30 (2004) 261–278.

[13] O.D. Nartey, B. Zhao, Biochar preparation, characterization, and adsorptive capacity and its effect on bioavailability of contaminants: an overview, Adv. Mater. Sci. Eng., 2014 (2014) 715398, doi: 10.1155/2014/715398.

[14] J. Lehmann, M.C. Rillig, J. Thies, C.A. Masiello, W.C. Hockaday, D. Crowley, Biochar effects on soil biota – a review, Soil Biol. Biochem., 43 (2011) 1812–1836.

[15] Z. Mahdi, A.E. Hanandeh, Q. Yu, Influence of pyrolysis conditions on surface characteristics and methylene blue adsorption of biochar derived from date seed biomass, Waste Biomass Valorization, 8 (2016) 2061–2073.

[16] R. Gokulan, G. Ganesh Prabhu, J. Jegan, A novel sorbent *Ulva lactuca*-derived biochar for remediation Remazol brilliant orange 3R in packed column, Water Environ. Res., 91 (2019) 642–649.

[17] R.P. Suresh Jeyakumar, V. Chandrasekaran, Preparation and characterization of activated carbons derived from marine green algae *Ulva fasciata* sp., Asian J. Chem., 26 (2014) 2545–2549.

[18] R. Gokulan, G. Ganesh Prabhu, J. Jegan, Remediation of complex Remazol effluent using biochar derived from green seaweed biomass, Int. J. Phytorem., 21 (2019) 1179–1189.

[19] R. Gokulan, A. Avinash, G. Ganesh Prabhu, J. Jegan, Detoxification of Remazol dyes by biochar derived from *Caulerpa scalpelliformis* - an eco-friendly approach, J. Environ. Chem. Eng., 7 (2019) 103297, doi: 10.1016/j.jece.2019.103297.

[20] P. Saha, S. Chowdhury, M. Tadashi, Insight into adsorption thermodynamic, Intechopen, 16 (2011) 349–364.

[21] M. Becidan, O. Skreiberg, J.E. Hustad, NOx and N$_2$O precursors (NH$_3$ and HCN) in pyrolysis of biomass residues, Energy Fuels, 21 (2007) 1173–1180.

[22] X. Tan, Y. Liu, G. Zeng, X. Wang, X. Hu, Y. Gu, Z. Yang, Application of biochar for the removal of pollutants from aqueous solutions, Chemosphere, 125 (2015) 70–85.

[23] G. Ravindiran, R. Jeyaraju, J. Josephraj, A. Alagumalai, Comparative desorption studies on remediation of Remazol dyes using biochar (sorbent) derived from green marine seaweeds, ChemistrySelect, 4 (2019) 7437–7445.

[24] Z. Aksu, S.S. Çagatay, Investigation of biosorption of Gemazol Turquise Blue-G reactive dye by dried *Rhizopus arrhizus* in batch and continuous systems, Sep. Purif. Technol., 48 (2006) 24–35.

[25] J. Tangaromsuk, P. Pokethitiyook, M. Kruatrachue, E. Upatham, Cadmium biosorption by *Sphingomonas paucimobilis* biomass, Bioresour. Technol., 85 (2002) 103–105.

[26] K. Vijayaraghavan, T. Ashokkumar, Characterization and evaluation of reactive dye adsorption onto biochar derived from *Turbinaria conoides* biomass, Environ. Prog. Sustainable Energy, 38 (2019) 13143, doi: 10.1002/ep.13143.

[27] T.V.N. Padmesh, K. Vijayaraghavan, G. Sekaran, M. Velan, Batch and column studies on biosorption of acid dyes on fresh water macro alga *Azolla filiculoides*, J. Hazard. Mater., 125 (2005) 121–129.

[28] M. Sathishkumar, A.R. Binupriya, K. Vijayaraghavan, S.I. Yun, Two and three-parameter isothermal modeling for liquid-phase sorption of Prociozn blue H-B by inactive mycelial biomass of *Panus fulvus*, J Chem. Technol. Biotechnol., 82 (2007) 389–398.

[29] M. Sathishkumar, S. Pavagadhi, K. Vijayaraghavan, R. Balasubramanian, S.L. Ong, Experimental studies on removal of microcystin-LR by peat, J. Hazard. Mater., 184 (2010) 417–424.

[30] T.J.M. Fraga, M.N. Carvalho, D.M.S.M. Fraga, M.C.L. da Silva, J.M. Ferreira, M.A.M. Sobrinho, Treated residue from aluminium lamination as adsorbent of toxic reactive dyes – a kinetic, equilibrium and thermodynamic study, Environ. Technol., 41 (2020) 669–681.

[31] E.H.C. de Oliveira, D.M.S.M. Fraga, M.P. da Silva, T.J.M. Fraga, M.N. Carvalho, E.M.P.L. Freire, M.G. Ghislandi, M.A.M. Sobrinho, Removal of toxic dyes from aqueous solution by adsorption onto highly recyclable xGnP® graphite nanoplatelets, J. Environ. Chem. Eng., 7 (2019) 103001, doi: 10.1016/j.jece.2019.103001.

[32] T.S. Pessoa, L.M.L. Ferreira, M.P. da Silva, L.M.P. Neto, B.F. do Nascimento, T.J.M. Fraga, E.F. Jaguaribe, J.V. Cavalcanti, M.A. da otta Sobrinho, Açaí waste beneficing by gasification process and its employment in the treatment of synthetic and raw textile wastewater, J. Cleaner Prod., 240 (2019) 118047, doi: 10.1016/j.jclepro.2019.118047.

[33] T.J.M. Fraga, L.F.F. da Silva, L.E.M. de Lima Ferreira, Amino-Fe$_3$O$_4$-functionalized multi-layered graphene oxide as an ecofriendly and highly effective nanoscavenger of the reactive drimaren red, Environ. Sci. Pollut. Res., 27 (2020) 9718–9732.

[34] T.M.N. de Paiva, T.J.M. Fraga, D.C.S. Sales, M.N. Carvalho, M.A.M. Sobrinho, *Anomalocardia brasiliana* shellfish shells as a novel and ecofriendly adsorbent of Nylosan Brilliant Blue acid dye, Water Sci. Technol., 78 (2018) 1576–1586.